Entry of Cholera Toxin into Polarized Human Intestinal Epithelial Cells

Identification of an Early Brefeldin A Sensitive Event Required for A_1-Peptide Generation

W. I. Lencer,*‖‡‡ J. B. de Almeida,‡ S. Moe,* J. L. Stow,‡ D. A. Ausiello,‡¶ and J. L. Madara§****

**Combined Program in Pediatric Gastroenterology and Nutrition, Children's Hospital; ‡Renal Unit, Massachusetts General Hospital; §Department of Pathology, Brigham and Women's Hospital; Departments of ‖Pediatrics, ¶Medicine, and **Pathology, Harvard Medical School; and ‡‡Harvard Digestive Diseases Center, Boston, Massachusetts 02115*

Abstract

The effect of brefeldin-A (BFA), a reversible inhibitor of vesicular transport, on cholera toxin (CT)-induced Cl^- secretion (I_{sc}) was examined in the polarized human intestinal cell line, T84. Pretreatment of T84 monolayers with 5 μM BFA reversibly inhibited I_{sc} in response to apical or basolateral addition of 120 nM CT (2.4±0.5 vs. 68±3 $\mu A/cm^2$, $n = 5$). In contrast, BFA did not inhibit I_{sc} responses to the cAMP agonist VIP (63±7 $\mu A/cm^2$). BFA had no effect on cell surface binding and endocytosis of a functional fluorescent CT analog or on the dose dependency of CT induced ^{32}P-NAD ribosylation of Gsα in vitro. In contrast, BFA completely inhibited (> 95%) the ability of T84 cells to reduce CT to the enzymatically active A_1-peptide. BFA had to be added within the first 10 min of CT exposure to inhibit CT-elicited I_{sc}. The early BFA-sensitive step occurred before a temperature-sensitive step essential for apical CT action. These studies show that sequential steps are required for a biological response to apical CT: (*a*) binding to cell surfaces and rapid endocytosis; (*b*) early, BFA-sensitive vesicular transport essential for reduction of the A_1-peptide; and (*c*) subsequent temperature-sensitive translocation of a signal (the A_1-peptide or possibly ADP-ribose-Gsα) to the basolateral domain. (*J. Clin. Invest.* 1993. 92:2941–2951.) Key words: cholera toxin • brefeldin A • vesicular transport • cell polarity • Cl^- secretion

Introduction

Secretory diarrhea caused by *Vibrio cholerae* is induced in large part by the direct action of cholera toxin (CT)[1] on polarized intestinal epithelial cells (1). The toxin elicits a secretory response directly by activating adenylate cyclase on the basolateral membrane of epithelial cells and indirectly by action on submucosal nerves (2) or other lamina propria cells (3). In intestinal crypt epithelia, toxin-induced activation of adenylate cyclase raises intracellular levels of cAMP which elicits the primary transport event of secretory diarrhea, electrogenic Cl^- secretion (4).

CT (84 kD) consists of 5 identical B-subunits (11 kD) which bind specifically to ganglioside G_{M1} on cell membranes and a single enzymatic A-subunit (28 kD) comprised of two peptides (23 kD and 5 kD) linked by a disulfide bond (5). In nature, the toxin binds by its B-subunits to ganglioside G_{M1} in the apical membrane of polarized intestinal epithelia but activates adenylate cyclase (6) on the cytoplasmic surface of the basolateral membrane (7, 8). Neither G_{M1} nor CT can pass through intercellular tight junctions (9, 10) and the mechanism by which apically bound CT transduces a signal to basolateral adenylate cyclase (or to submucosal tissues) remains undefined.

CT-induced activation of adenylate cyclase occurs only after an unexplained "lag phase" of 10–40 min after binding to the cell surface (11). Studies on a variety of nonpolarized cells have shown that during this lag phase, the A-subunit translocates across the plasma membrane (or possibly across the endosome membrane [12]) to the cytoplasmic membrane surface (13, 14, 15). During or after translocation, the A-subunit undergoes reductive cleavage to form the enzymatically active A_1-peptide (13). Whether the A_1-peptide dissociates completely from the B-subunit or from the cell membrane after translocation remains undefined. Eventually, the A_1-peptide gains access to and catalyses the ADP-ribosylation of the heterotrimeric G-protein, Gsα, which leads to activation of adenylate cyclase (16, 17). It is not known where in the cell translocation of the A-subunit occurs or where the A_1-peptide encounters Gsα. Furthermore, in polarized epithelia, where the apical toxin binding site is separated from basolateral adenylate cyclase by circumferential tight junctions, it is not known whether the A_1-peptide itself or rather ADP-ribosylated-Gsα moves to the basolateral membrane, thus linking the apical signal with the basolateral effector (7, 18, 19). Previous studies in nonpolarized cells have shown that CT is internalized by receptor-mediated endocytosis (20, 21, 22) but whether endocytosis and vesicular traffic of toxin-containing membranes plays any role in signal transduction was not examined directly.

We have recently defined the human intestinal cell line T84 as a model to study the mechanism of CT action on polarized epithelia (19). T84 cells grown as confluent monolayers on permeable supports display features of intestinal crypt cells and respond to CT with cAMP-dependent Cl^- secretion that can be detected electrically with a high degree of sensitivity and temporal resolution. This system is particularly relevant because the model requires that CT transduce a signal from the apical (physiologic) membrane and the response to CT in T84 cells reproduces the primary transport event of secretory diarrhea in humans. Utilizing this model system we have shown that CT-

Address correspondence to Dr. W. I. Lencer, Combined Program in Pediatric Gastroenterology and Nutrition, Children's Hospital, 300 Longwood Avenue, Boston, MA 02115.

Received for publication 27 April 1993 and in revised form 6 August 1993.

1. *Abbreviations used in this paper:* A_1, CT-A_1-peptide; AC, adenylate cyclase; ARF, ADP-ribosylating factor; BFA, brefeldin A; CT, cholera toxin; Gsα, hetertrimeric GTPase Gsα; PKA, protein kinase.

J. Clin. Invest.

0021-9738/93/12/2941/11 $2.00
Volume 92, December 1993, 2941–2951

induced signal transduction from the apical cell surface involves endocytosis and vesicular transport of toxin-containing (and possibly ADP-ribose-Gsα-containing) membranes. Both a longer lag phase and an essential temperature-dependent step were required for signal transduction by apical, but not basolateral CT. This temperature-sensitive step occurred late in the lag phase after endocytosis of CT-containing membranes and after formation of the A_1-peptide. The data indicate that at this late stage in the lag phase, the A_1-peptide (or possibly ADP-ribose Gsα) must remain membrane-associated or tethered to other structural elements because subsequent activation of adenylate cyclase was not diffusion limited at nonpermissive temperatures (19). These data strongly suggest that the mechanism of toxin action from the apical membrane of polarized epithelia involves endocytosis of CT and at least one additional vesicular transport event not required if CT is exposed directly to the basolateral membrane of the same cell.

Our aim in the present study was to define the effect of brefeldin A (BFA) on CT action in the polarized T84 cell model. BFA is a fungal metabolite known to interfere with vesicular transport in the endosomal (23, 24), transcytotic (25), and exocytotic (26) pathways of many eukaryotic cells (27, 28). During the course of peer review of this manuscript, two studies from separate laboratories report effects of BFA on CT action in nonpolarized cell systems (29, 30). Here, we find that BFA inhibits CT-induced Cl^- secretion from polarized T84 cells by reversibly blocking an event which occurs after endocytosis of CT-containing membranes but before formation of the A_1-peptide. Moreover, this early lag phase brefeldin A-sensitive event(s) can be clearly distinguished from the late lag phase temperature-sensitive event required for toxin-action from the apical cell surface (19). Lastly, we find that signal transduction by apical CT involves additional (or different) steps that are more sensitive to BFA and of longer duration than that required for signal transduction by basolateral CT. These data strongly support a role for multi-compartmental vesicular transport of toxin-containing membranes in the mechanism of CT-action on polarized intestinal epithelia.

Methods

Materials. CT was obtained from Calbiochem-Novabiochem Corp. (San Diego, CA), Na ^{125}Iodine and nicotinamide adenine dinucleotide, di(triethylammonium) salt [adenylate-^{32}P]-(^{32}P-NAD) from New England Nuclear (Boston, MA), and brefeldin A from Epicentre Technologies (Madison, WI). All other reagents were from Sigma Chemical Co. (St Louis, MO) unless otherwise stated. HBSS (containing in g/liter 0.185 $CaCl_2$, 0.098 $MgSO_4$, 0.4 KCl, 0.06 KH_2PO_4, 8 NaCl, 0.048 Na_2HPO_4, 1 glucose, to which was added 10 mM Hepes, pH 7.4) was used for micro-assay of Cl^- secretion, measurement of A_1-peptide formation, morphologic studies, and quantitation of A_1-peptide.

Cell culture. T84 cells obtained from American Type Culture Collection (Rockville, MD), were cultured and passaged as previously described (31) in equal parts of DME (1 g/liter D-glucose) and Ham's F-12 Nutrient mixture, supplemented with 5% newborn calf serum, 15 mM Hepes, 14 mM $NaHCO_3$, 40 mg/liter penicillin, 8 mg/liter ampicillin, and 0.90 mg/liter streptomycin. Cells were seeded at confluent density onto glass coverslips, or 5 cm^2 or 0.33 cm^2 Transwell inserts (Costar, Cambridge, MA) coated with a dilute collagen solution as previously described (32). Transepithelial resistances attained stable levels (> 1,000 ohms/cm^2) after 7 d. The development of high transepithelial resistance correlated with the formation of confluent monolayers with well-developed tight junctions as assessed by morphological analysis (33), and with the ability of monolayers to secrete Cl^-. Cells from passages 62 to 72 were utilized for these experiments.

Electrophysiology. For electrophysiological studies, confluent monolayers on Transwell inserts were transferred to HBSS. Measurements of short circuit current (I_{sc}) and resistance (R) were performed with 5 cm^2 or 0.33 cm^2 monolayers as previously described (19, 31, 32). Serosal and mucosal reservoirs were interfaced with calomel and Ag-AgCl electrodes via 5% agar bridges made with Ringers buffer (114 mM NaCl, 5 mM KCl, 1.65 mM Na_2HPO_4, 0.3 mM NaH_2PO_4, 25 mM $NaHCO_3$, 1.1 mM $MgSO_4$, 1.25 mM $CaCl_2$). Measurements of resistance were made using a dual voltage/current clamp device (University of Iowa) and 100 or 25 μA current pulses. Short circuit current (I_{sc}) was calculated using Ohm's law.

Quantitation of reduction of A-subunit after binding of CT to T84 cells. ^{125}I-labeled CT was prepared as previously described (34) and had a specific activity of 200–400 cpm/fmole and a half-maximal effective dose (ED_{50} = 500–800 pM) identical to that of native toxin when applied to apical surfaces of T84 monolayers. Reduction of the A-subunit to the A_1-peptide was assessed using modifications of methods described by Kassis (13) and LeBivic (35). T84 monolayers (5 cm^2 inserts) were incubated with 40 nM ^{125}I-labeled CT in HBSS applied apically or basolaterally at 4°C for 30 min, washed, and shifted to 37°C for 1 h. Incubations were stopped by immersion into HBSS containing 10 mM *N*-ethylmaleimide (Calbiochem-Novabiochem Corp.) at 4°C for at least 15 min. Total cell extracts were prepared by excising monolayers and their filters from the inserts and immersing them into 600 μl SDS-lysis buffer (0.5% SDS, 20 mM Tris, 150 mM NaCl, 5 mM EDTA, 20 mM triethanolamine, 10 mM *N*-ethylmaleimide, 1 mM PMSF, and 10 μg/ml chymostatin, pH 7.4) followed by treatment with 2.5 μM diisopropylfluorophosphate and incubation at 65°C for 5 min. The extract was then returned to 4°C and diluted 1:1 (vol/vol) with triton dilution buffer (2.5% triton-X 100, 20 mM Tris, 150 mM NaCl, 5 mM EDTA, 20 mM triethanolamine, 10 mM *N*-ethylmaleimide, 1% Na Azide, 1 mM PMSF, and 10 μg/ml chymostatin, pH 7.4).

After shearing the DNA by vortex and needle aspiration, the A-subunit and A_1-peptide were immunoprecipitated using 20 μl (1:600 final dilution) polyclonal antiserum raised against heat and SDS-denatured CT A-subunit followed by 150 μl protein-A sepharose. The protein-A beads were washed three times with mixed micelle buffer (1% triton-X 100, 0.2% SDS, 8% sucrose, 20 mM Tris, 150 mM NaCl, 5 mM EDTA, 20 mM Triethanolamine, 10 mM *N*-ethylmaleimide, 1% NaAzide, 1 mM PMSF, and 10 μg/ml chymostatin, pH 7.4) and once with final wash buffer (8% sucrose, 20 mM Tris, 150 mM NaCl, 5 mM EDTA, 20 mM Triethanolamine, 10 mM *N*-ethylmaleimide, 1% NaAzide, 1 mM PMSF, and 10 μg/ml chymostatin, pH 7.4). The pelleted beads were resuspended in 150 μl sample buffer (4% SDS, 8 M urea, 5 mM EDTA, 10 mM NEM, 0.34 M sucrose), heated to 65°C for 5 min and repelleted. 50–80% of radioactivity contained in the final lysate was recovered. The supernatants were run on nonreducing 12% SDS-polyacrylamide gels. The gels were stained and fixed with Coomassie blue, destained, and each lane was cut into 1-mm slices. Total radioactivity in slices was quantified by gamma counting, and radioactive peaks corresponding to A- and A_1-subunits were identified. The fractional component of A_1-peptide was defined as the ratio of A_1- to A-band integrals as previously described (19).

Conventional and confocal fluorescence microscopy. Binding and internalization of CT in T84 cell monolayers were visualized using rhodamine-labeled (CT-rhodamine) and fluorescein-labeled (CT-fluorescein) toxin analogs, prepared as previously described (19). CT-rhodamine was functionally active with an ED_{50} identical to native toxin. CT-fluorescein did not elicit a secretory response from T84 cells but bound specifically to ganglioside GM1 as assessed by morphology. After incubation with 20 mM CT-fluorescein or CT-rhodamine at 4°C or 37°C, T84 monolayers were washed three times in HBSS at 4°C, fixed in a solution of 4% paraformaldehyde and 5% sucrose in PBS (150 mM NaCl, and 20 mM NaH_2PO_4/Na_2HPO_4, pH 7.4) for 30 min at 4°C, rinsed in PBS, and mounted in 1:1 PBS/glycerol containing 1% *n*-propyl gallate. Monolayers grown on filter supports were excised

from the plastic insert, mounted in PBS/glycerol as above, and examined using a Zeiss Axiophot photomicroscope (Carl Zeiss, Oberkochen, Germany) equipped with an argon laser and Biorad MRC600 confocal imaging system (BioRad/Analytical Instruments Corp., Cambridge, MA). Monolayers grown on glass coverslips were mounted in PBS/glycerol as above or in Moviol (Hoechst AG, Basel, Switzerland) and examined using a Zeiss Axiophot photomicroscope equipped with a 546±12 nm narrow band pass excitation filter and a 590-nm-long pass barrier filter. Photographs were taken using T-Max 400 film (Eastman Kodak Co., Rochester, NY).

For immunocytochemical localization of the Golgi associated protein p200 (36), monolayers grown on glass coverslips were incubated in HBSS with and without BFA for 30 min at 37°C and fixed as described above. The fixed monolayers were permeabilized by incubation in 1% Triton X-100 in PBS for 20 min at 21°C, and then washed extensively in PBS containing 1% BSA (PBS/BSA). Mouse mAbs against the Golgi protein p200 (obtained from Dr. Brian Burke, Harvard Medical School, Boston) were diluted 1:1,000 in PBS/BSA and applied to the permeabilized monolayers. Bound antibodies were visualized by subsequent incubation with rhodamine-labeled goat anti-mouse IgG (Cappel Laboratories, Corp., Durham, NC). Monolayers were mounted and photographed as described above.

Preparation of T84 cell membrane and cytosol fractions. T84 cell membranes and cytosol were prepared by differential centrifugation as described by Kaoutzani (37). Briefly, T84 cells were scraped into homogenization buffer (0.34 mM sucrose, 10 mM Hepes, 1 mM EDTA, 0.1 mM $MgCl_2$), lysed by nitrogen bomb (200 psi for 15 min), treated with 2.5 μM diisopropylfluorophosphate, and centrifuged at 1,000 *g* for 20 min to remove nuclei and unbroken cells. The resulting supernatant was centrifuged at 100,000 *g* for 1 h to obtain a crude postnuclear cell pellet (~ 1.5 mg/ml protein) and supernatant (~ 0.2 mg/ml protein).

ADP-Ribosylation of Gsα. CT-induced ADP-ribosylation of T84 cell membranes was performed using modifications of the protocol described by Ribeirto-Neto (38). Briefly, 20 μgm T84 cell membranes were incubated for 3 h at 4°C with sequential 10-fold dilutions of CT (as indicated) and 300 mM KH_2PO_4/K_2HPO_4 (from 2.4 M stock prepared at pH 7.0), 12.5 mM tris-base (adjusted to pH 7.5), 10 mM thymidine, 10.5 mM $MgCl_2$, 1 mM EDTA, 1 mM ATP, 0.1 mM GTP, 0.8% lubrol-Px, and 60 μM NAD (containing 2 μCi ^{32}P-labeled NAD/sample as tracer) in a total volume of 120 μl. The reaction was stopped by the addition of 1 ml ice cold trichloroacetic acid followed by centrifugation at 14,000 *g* for 15 min. The pellets were washed in 1 ml ice cold ether, centrifuged again, and resuspended in 30 μl SDS-sample buffer. Membrane proteins were resolved by SDS-PAGE and autoradiographed.

Statistics. BFA effects on CT-induced Cl^- secretion and formation of A_1-peptide were analyzed by *t* test and ANOVA using Statview 512+ software (Brainpower, Inc., Calabasas, CA).

Results

Cholera toxin-induced Cl^- secretion is inhibited reversibly by brefeldin A. Pretreatment of T84 monolayers with 5 μM BFA at 37°C 10 min before the addition of CT (120 nM) completely inhibited the secretory response to CT applied either to apical or basolateral cell surfaces (peak I_{sc} for apical CT: 2.4±0.5 vs. 68±3 μA/cm^2; peak I_{sc} for basolateral CT: 2.9±0.5 vs. 74±3 μA/cm^2, mean±SEM, n = 5, P = 0.0001 respectively) (see Fig. 1 *A*). In contrast, BFA had no effect on the secretory response to the cAMP agonists 1 nM vasoactive intestinal peptide (VIP), 1 μM forskolin, or 3 mM 8Br-cAMP (Fig. 1 *B*). The time course of toxin-induced Cl^- secretion (0.5 nM CT) in the presence and absence of BFA (5 μM) and after BFA removal is shown in Fig. 2. Monolayers exposed to apical CT in the absence of BFA elicited a strong secretory response after a 45±2 min lag phase (peak I_{sc} = 22±1.8 μA/cm^2, mean±SEM, n = 6). In contrast, toxin-induced Cl^- secretion was completely inhibited in those monolayers pretreated with BFA (apical CT: I_{sc} = 1.7±0.3 μA/cm^2, mean±SEM, n = 4; basolateral CT: I_{sc} = 2.5±0.5 μA/cm^2, n = 6). Removing BFA by exchanging reservoir buffers at 100 min ("wash" arrow, Fig. 2) permitted recovery of toxin induced Cl^- secretion after an additional 88±3 min for apical CT (peak I_{sc} = 10.9±0.3 μA/cm^2, mean±SEM, n = 4) and 70±3 min for basolateral CT (peak I_{sc} = 19±1.1 μA/cm^2; n = 6). In contrast, exchanging reservoir buffers had no effect on I_{sc} in control monolayers not exposed to CT whether treated or not treated with BFA (1.3±0.2 and 1.4±0.4 μA/cm^2, mean±SEM, n = 2). The viability of these

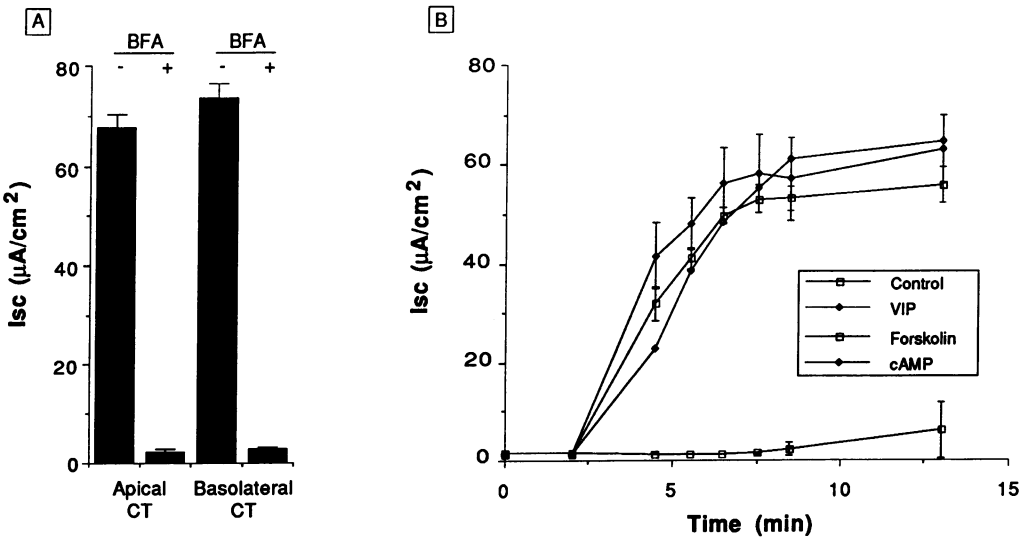

Figure 1. Brefeldin A completely inhibits CT-induced Cl^- secretion but does not affect the secretory response to other cAMP-agonists. (*A*) Peak I_{sc} elicited by apical or basolateral CT (120 nM, at 110 min) in the presence and absence of 5 μM brefeldin A, mean±SEM, n = 5. CT induced Cl^- secretion was completely inhibited in monolayers pretreated with BFA. (*B*) Time course of Cl^- secretion after administration of either 1 nM VIP, 1 μM forskolin, 3 mM 8 Br-cAMP, or buffer alone to serosal reservoirs in the presence of 5 μM BFA. While toxin-induced Cl^- secretion was completely inhibited by BFA (dI_{sc}/dt = not present; peak I_{sc} = 2.4±0.5 μA/cm^2, mean±SD, n = 3) neither receptor-mediated activation of $G_{s\alpha}$ (VIP: dI_{sc}/dt = 16 μA/cm^2/min; peak I_{sc} = 63±5.4 μA/cm^2, n = 2), nor direct activation of adenylate cyclase (forskolin: dI_{sc}/dt = 12.2 μA/cm^2 per min; peak I_{sc} = 56±3.5 μA/cm^2) or protein kinase-A (cAMP: dI_{sc}/dt = 10.3 μA/cm^2 per min; peak I_{sc} = 65±11.8 μA/cm^2) were rate limiting in the presence of BFA. I_{sc} responses to these agonists do not significantly differ from those in the absence of BFA.

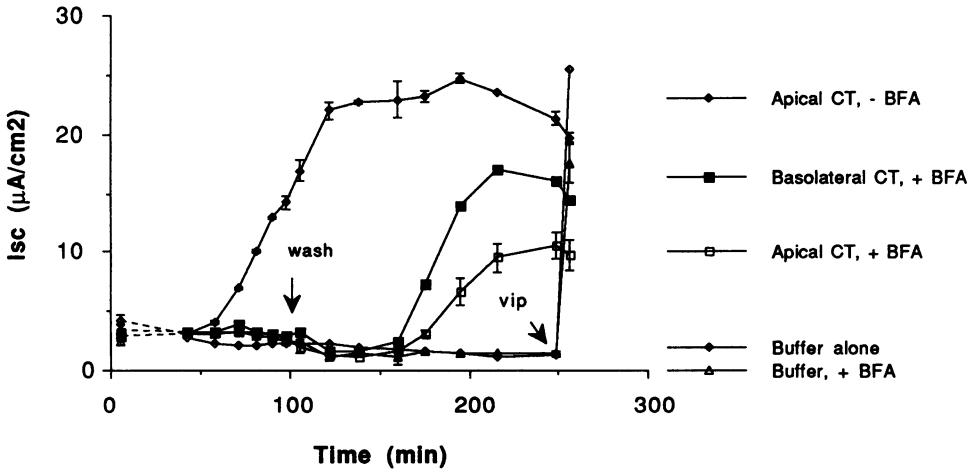

Figure 2. BFA reversibly inhibits CT-induced Cl^- secretion. Time course of Cl^- secretion elicited by 0.5 nM CT applied to apical (*filled diamond and open square*) or basolateral (*filled square*) surfaces of T84 monolayers in the presence or absence of 5 μM BFA. After a 45-min lag, T84 monolayers not treated with BFA (*filled diamond*) respond to apical CT with a strong secretory response. In contrast, the secretory response to both apical and basolateral CT was completely inhibited in monolayers treated with BFA. To examine whether inhibition was reversible, BFA was removed by exchanging reservoir buffers at 100 min (*wash arrow*), which led to CT-induced Cl^- secretion in monolayers exposed to apical (*open square*) or basolateral CT (*filled square*). Washing had no effect on control monolayers not exposed to CT (*open diamond and open triangle*). To demonstrate the viability of these controls, 1 nM VIP was added to serosal reservoirs at 250 min.

control monolayers was demonstrated by the brisk secretory response elicited by the addition of VIP at 250 min (dI_{sc}/dt = 2.0±0.6 μA/cm²/min; peak I_{sc} = 22.4±2.5 μA/cm²).

These data show that the secretory response to CT applied to either apical or basolateral cell surfaces was completely and reversibly inhibited by treatment with 5 μM BFA. In contrast, brefeldin had no effect on Cl^- secretion induced by receptor-mediated activation of $G_{s\alpha}$ (VIP), or direct activation of adenylate cyclase (forskolin) or protein kinase-A (8Br-cAMP). Furthermore, though BFA may induce cation selective channels when added to artificial lipid bilayers (39), the drug did not affect membrane or transepithelial potentials in the T84 cell system.

Toxin-induced signal transduction and cell polarity. We next examined the time and dose dependency of BFA action. To determine when the rate-limiting BFA-sensitive event occurred in the complex sequence of events leading to toxin-induced Cl^- secretion (Fig. 3), monolayers were incubated with CT at 4°C for 30 min (to allow steady-state binding to cell surfaces) and then shifted to 37°C, which defined the beginning of the lag phase. The monolayers were then either treated with BFA (5 μM) at the onset of the lag phase (at time 0 min), at sequential points throughout the lag phase (at 1, 2.5, 5, 10, etc., min), or not treated with BFA. When cholera toxin was applied to apical cell surfaces, BFA completely inhibited toxin induced Cl^- secretion only if it were added within the first 10 min of the lag phase (Fig. 3, *hatched bars*). In monolayers exposed to basolateral toxin, however, BFA did not completely inhibit a secretory response unless applied within the first minute (Fig. 3, *solid bars*). Thus, the entire fraction of apical toxin remained in a BFA-sensitive compartment(s) for at least 5 min while a small fraction of basolateral CT had already moved beyond a BFA-sensitive step within 1 min after the monolayers were shifted to permissive temperatures. Apparent half-times for transit through the BFA-sensitive compartment(s) were 20 min from the apical membrane and 10 min from the basolateral membrane (n = 4, two-tailed t-test, P = 0.001).

The importance of cell polarity in toxin-induced signal transduction was further emphasized by small but reproducible differences in the dose dependency of BFA inhibition (Fig. 4). The Cl^- secretory response in monolayers exposed to apical CT were twofold more sensitive to BFA than in monolayers exposed to basolateral CT (ED_{50} = 55 vs. 90 nM, mean, n = 2). Taken together, these studies show that the cellular processing of both apical and basolateral CT was sensitive to BFA if applied early in the lag phase, and that the mechanism of toxin action from the apical cell surface involved additional (or different) steps that were more sensitive to BFA and longer in duration.

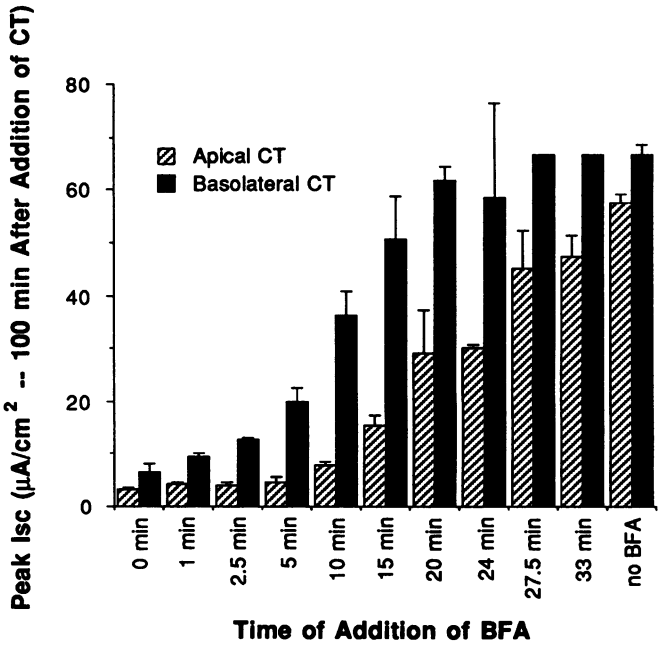

Figure 3. BFA inhibits an early event in the lag phase. Monolayers were initially treated with 120 nM CT applied to apical (*hatched bars*) or basolateral (*filled bars*) cell surfaces at 4°C for 30 min. BFA (5 μM) was added to apical and basolateral reservoirs at the indicated times after shifting the monolayers to permissive temperatures (37°C). Peak I_{sc} at 110 min (mean±SE, n = 4) is plotted on the vertical axis against the time of treatment with 5 μM BFA on the horizontal axis. Lag phase duration in the absence of BFA was 43 min for apical CT (120 nM) and 32 min for basolateral CT.

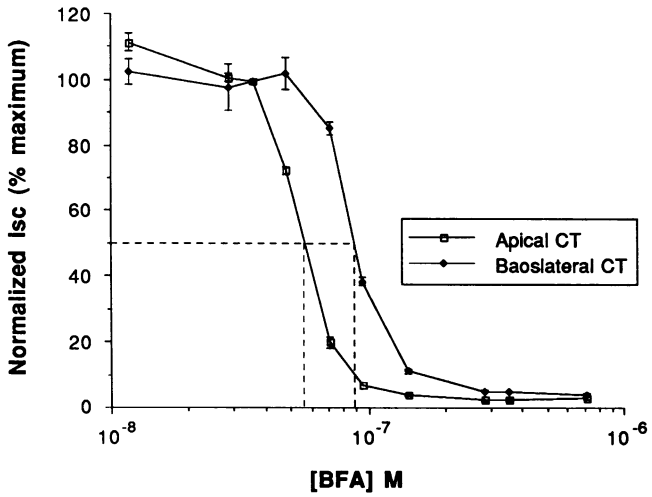

Figure 4. Dose dependency of BFA-inhibition. Monolayers were exposed to either 120 nM CT at the apical (*open squares*) or basolateral (*filled diamonds*) cell surface. I_{sc} at 110 min (mean±SD, $n = 2$) was normalized to peak I_{sc} elicited by apical or basolateral CT in the absence of BFA. Monolayers exposed to apical CT were approximately twofold more sensitive to BFA. Data represents one of two independent experiments each performed in duplicate.

Mechanism of CT action: identification of the BFA-sensitive event. For CT to act directly from either the apical or basolateral membrane, the toxin must first bind specifically to ganglioside G_{M1} on the cell surface, the A-subunit must translocate across the membrane and undergo reductive cleavage to form the enzymatically active A_1-peptide, and the A_1-peptide must eventually catalyze the ADP-ribosylation of the heterotrimeric GTPase, Gsα, which activates adenylate cyclase. These events are measurable landmarks that can serve to delineate potential sites of BFA-sensitivity.

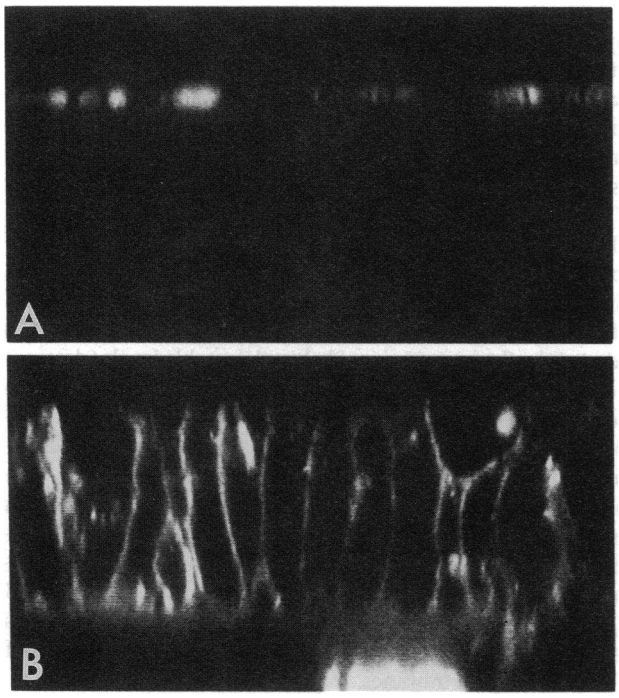

Figure 5. Confocal epifluorescence micrograph of T84 monolayers treated with 5 μM BFA and exposed to 20 nM CT-fluorescein at the apical (*A*) or basolateral (*B*) cell surface. One of three independent experiments.

To examine the possible effect of BFA on CT binding to cell surfaces, the fluorescent toxin analog CT-fluorescein (10 nM) was applied to apical or basolateral reservoirs of T84 monolayers and visualized by laser confocal microscopy. When applied to apical reservoirs at 4°C in the presence of BFA (5 μM), a bright fluorescent signal was apparent at apical cell surfaces (Fig. 5 *A*). Fluorescence was not detected either within T84 cells or on the contralateral cell surface, indicating both that endocytosis was effectively inhibited at 4°C and little, if any, CT-fluorescein passed through tight junctions by a paracellular route. Similarly, when applied to basolateral reservoirs at 4°C in the presence of BFA, CT-fluorescein outlined basolateral cell surfaces with no detectable signal within the cell or at the apical membrane (Fig. 5 *B*). The fluorescent signals were completely inhibited by co-incubation with 100-fold excess unlabeled (nonfluorescent) CT indicating that the binding was specific and receptor mediated. These data show that BFA did not inhibit the specific binding of CT-fluorescein to either apical or basolateral plasma membranes.

A possible direct effect of BFA on CT-catalyzed ribosylation of Gsα was examined in crude T84 cell membrane preparations (100,000 *g* postnuclear cell pellets) incubated in vitro with serial 10-fold dilutions of CT (10^{-6} to 10^{-12} M) and 2 μCi ^{32}P-labeled NAD in the presence or absence of 1 mM BFA (> 10^4-fold excess over IC_{50} for intact cells). Membrane proteins were separated by SDS-PAGE and autoradiographed (Fig. 6). CT preferentially catalyzed the ADP-ribosylation of two membrane proteins with apparent mol mass of 45 and 52 kD (arrowheads), both of which were immunoreactive with antibodies against Gsα as assessed by western blot (data not shown). The CT-catalyzed ADP-ribosylation of these protein bands displayed an identical dose dependency in the presence or absence of BFA over three orders of magnitude (10^{-6}–10^{-8}). These data indicate that in membrane fractions, where spatial restrictions on the ability of CT to interact with its substrate are not rate limiting, BFA had no effect on the ability of CT to ADP-ribosylate Gsα.

To examine the possibility that BFA might affect reductive cleavage and presumably translocation (13) of the A-subunit by intact T84 cells, we assessed the degree of reduction of CT to the A_1-peptide after application of the toxin to apical cell surfaces in the presence or absence of BFA (5 μM). ^{125}I-labeled CT (20–40 nM) was applied to the apical surfaces of T84 monolayers at 4°C for 30 min. Monolayers were then either warmed to 37°C for 60 min in the presence or absence of BFA or kept at 4°C to define background levels of A-subunit reduction. Reduction of the A-subunit was detected by the appearance of radiolabeled A_1-peptide that is shifted in electrophoretic mobility on non-reducing polyacrylamide gels. Fig. 7 summarizes the results (mean±SEM, $n = 3$) of these experiments. After 1 h at 37°C, T84 monolayers not treated with BFA produced nearly twofold more A_1-peptide (12±1.4%) than control monolayers kept at 4°C (6.4±0.6%) (ANOVA, $P < 0.007$). In contrast, the fraction of A_1-peptide produced by monolayers incubated at 37°C in the presence of BFA (6.5±0.3%) was no different than that seen in 4°C controls.

To determine if BFA directly inhibited reduction of the A-subunit in vitro, CT (1 mg/ml) was mixed (1:20 vol/vol)

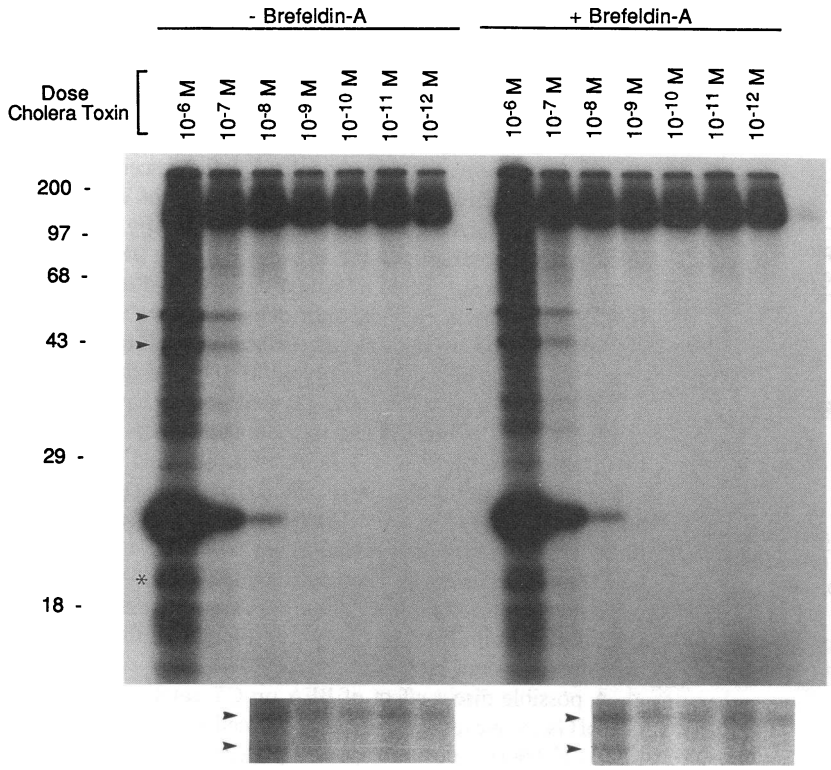

Figure 6. Autoradiograph (20-h exposure) of T84 cell pellets (100,000 *g*) incubated with 10-fold serial dilutions of CT (10^{-6} to 10^{-12} M) in the presence and absence of 1 mM BFA and 2 μCi ^{32}P-NAD (60 μM NAD). Arrowheads at 52 and 45 kD mark protein bands (presumably Gsα) that were preferentially ADP-ribosylated by CT. Insets below show the 7-d exposure of lanes labeled 10^{-8} to 10^{-12} M CT to illustrate the specific CT-catalyzed ADP-ribosylation of the 52- and 45-kD proteins at 10^{-8} M CT. CT-catalyzed ADP-ribosylation of the 45-kD protein was not present at 10^{-9} to 10^{-12} M CT. CT-catalyzed ADP-ribosylation of Gsα displayed an identical dose dependency over three orders of magnitude in the presence and absence of BFA. Auto-ADP-ribosylation of the A-subunit is apparent at 23 kD. The heavily labeled band at the top of each lane is poly ADP-ribose. * marks a 20-kD protein ADP-ribosylated by CT at 10^{-6} and 10^{-7} M (see Discussion). Data shown represent one of two independent experiments with identical results.

with crude T84 cytosol (~ 0.2 mg protein/ml) or postnuclear membrane fractions (~ 1 mg protein/ml) and incubated at 37°C for 5 min. In the presence of either T84 cytosol or postnuclear membrane fractions 50 to > 90% of the A-subunit was reduced to the A_1-peptide. These data indicate that BFA did not affect reduction of the A-subunit in cell fractions where there were no spatial restrictions on the ability of CT to interact with its substrates. In contrast, the drug completely blocked formation of the A_1-peptide when applied to intact cells. Taken together, these studies strongly suggest that BFA inhibited CT-action on intact cells by blocking the transport of CT-containing membranes into a compartment where reduction and presumably translocation of the A-subunit occurs.

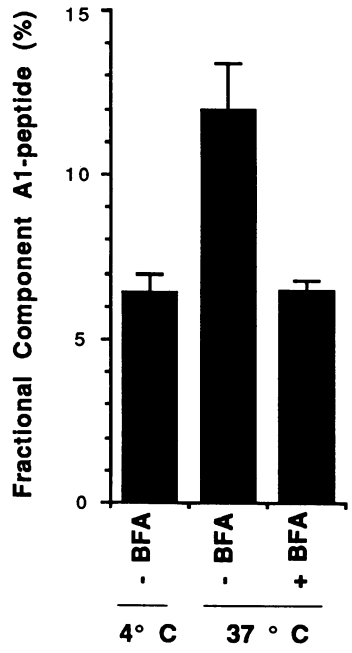

Figure 7. BFA effect on reduction of apical ^{125}I-CT to the A_1-peptide by T84 cells. After 1 h at 37°C in the absence of BFA, the fraction of A-subunit reduced to the A_1-peptide was almost twofold greater than background (1 h at 4°C) (mean±SEM, n = 3, ANOVA, P = 0.007). In contrast, after 1 h at 37°C in the presence of 5 μM BFA, the fraction of A-subunit reduced to the A_1-peptide was no different than background. BFA completely inhibited the ability of intact T84 monolayers to reduce CT to the A_1-peptide.

Endocytosis of CT-containing membranes and Golgi structure in the presence of BFA. We have previously shown that toxin-induced signal transduction from the apical membrane of T84 cells requires entry of CT into the apical endosomal compartment (19). To examine whether BFA inhibited toxin action by affecting endocytosis of toxin-containing membranes, the functional fluorescent-toxin analog CT-rhodamine was visualized directly within T84 cells by conventional epifluorescence microscopy. T84 monolayers grown on glass coverslips were incubated with CT-rhodamine (20 nM) at 4° or 37°C for 40 min in the presence (or absence) of BFA. At 4°C, CT-rhodamine was visualized in a pattern consistent with toxin binding to apical cell surfaces (Fig. 8 *A*). Competition with 50-fold excess nonfluorescent CT (10 min preincubation followed by 40 min co-incubation with CT-rhodamine at 4°C) reduced the fluorescent signal below detectable levels (data not shown) indicating that binding was specific (Fig. 8 *B*). When monolayers were incubated at 37°C (for 40 min) in the presence of BFA, CT-rhodamine was visualized within intracellular structures of nearly all cells in a pattern consistent with endocytic uptake (Fig. 8 *C*). Competition with 100-fold excess nonfluorescent-CT (10 min preincubation followed by continuous 40-min co-incubation with CT-rhodamine at 37°C) completely eliminated the labeling of intracellular structures (Fig. 8 *D*), confirming that internalization in BFA-treated cells was also receptor mediated. Thus BFA did not affect endocytosis of CT-containing membranes.

To determine whether Golgi structure in T84 cells was sensitive to BFA, we examined whether treatment with BFA caused a redistribution of the Golgi associated protein p200 as assessed by immunocytochemistry. Dissociation of p200 from

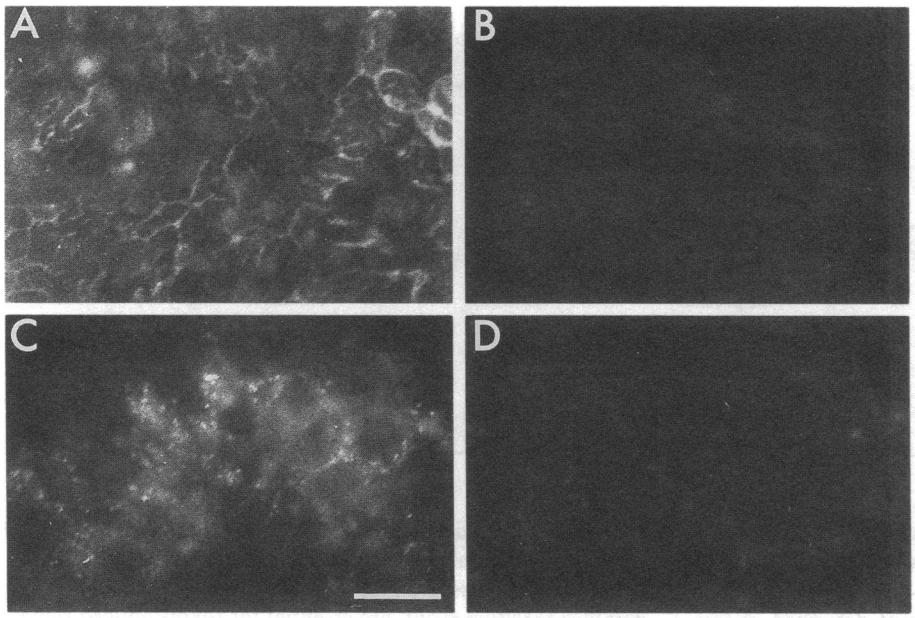

Figure 8. BFA does not inhibit endocytosis of CT by T84 cells. T84 monolayers grown on glass coverslips were exposed to 20 nM CT-rhodamine in the presence of BFA (5 μM) for 40 min at 4°C (*A* and *B*) or at 37°C (*C* and *D*). Monolayers shown in *B* and *D* were incubated with CT-rhodamine in the presence of excess competing nonfluorescent CT (1 μM). The monolayers were viewed enface by epifluorescence microscopy. At 4°C (*A*), CT-rhodamine binds to apical membranes and highlights large microvillar folds of the apical cell surface. Basolateral membranes are not labeled and the boundaries between cells are not apparent. (*C*) Shows a cluster of cells growing at the edge of a larger colony. After 40 min at 37°C, CT-rhodamine labels intracellular structures in a pattern consistent with endocytic uptake. The location and size of nuclei of individual cells can be appreciated due to fluorescence from internalized toxin. Co-incubation with excess nonfluorescent toxin (*B* and *D*) decreases the fluorescent signal below detectable levels indicating that both binding to the apical cell surface at 4°C and endocytosis at 37°C are specific and receptor mediated. Bar, 5 μm.

Golgi membranes occurs rapidly upon exposure to BFA and precedes gross disruption of Golgi morphology (36). We found that in T84 cells not treated with BFA mAbs against p200 labeled perinuclear structures consistent with the location of Golgi stacks (data not shown). These structures were not labeled in monolayers treated with BFA for 45 min before fixation (ED50 ~ 100 nM) or in control monolayers that were fixed but not permeabilized before incubation with antibodies against p200. Taken together, these data indicate that Golgi structure, as assessed by localization of the coat protein p200, was sensitive to BFA, but endocytosis of CT-containing membranes from the cell surface was not.

Two sequential and distinct events involving vesicular transport are required for signal transduction from the apical cell surface. We have previously shown that the ability of apical CT to elicit Cl^- secretion in T84 cell monolayers involved a temper-

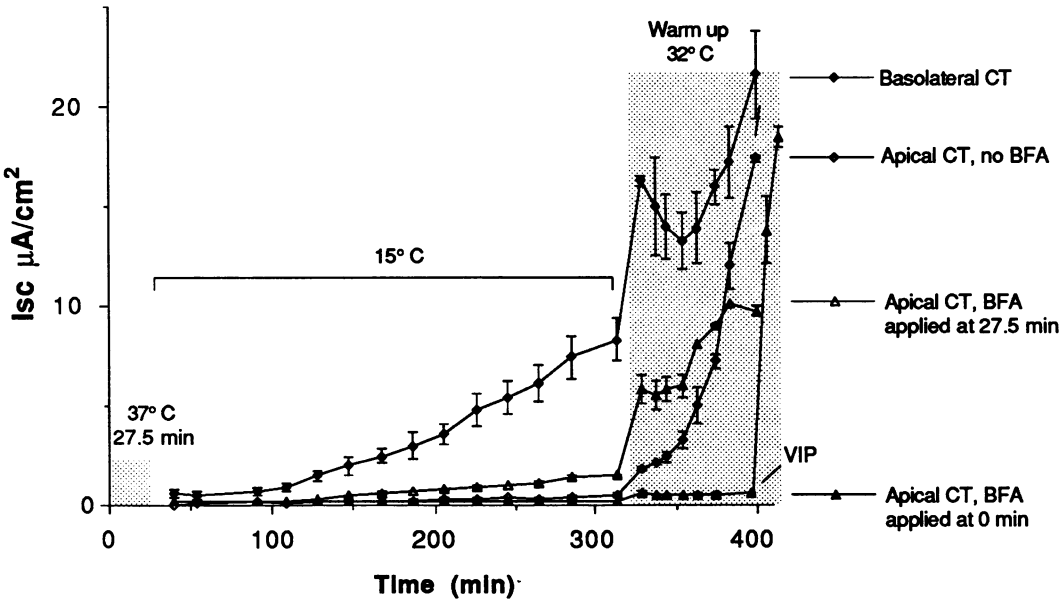

Figure 9. Signal transduction by apical CT involves distinct BFA-sensitive and temperature-sensitive events. Time course of CT-induced Cl^- secretion after basolateral (*filled diamond*) or apical application of 120 nM CT at 4°C, preincubation at 37°C for 27.5 min, and then returning monolayers to 15°C. Monolayers exposed to apical CT were either treated with 5 μM BFA early in the lag phase (at 0 min, *filled triangle*), late in the lag phase (at 27.5 min, *open triangle*), or not treated with BFA (*open diamond*). Shaded areas indicate where monolayers were rewarmed to 32°C. Preincubation of monolayers for 27.5 min overcame the temperature block for basolateral but not apical CT. Rewarming to 32°C at 325 min released the temperature block and elicited a secretory response in monolayers exposed to apical CT and treated with BFA late in the lag phase (*open triangle*) or not treated with BFA (*open diamond*). In contrast, rewarming did not elicit a secretory response in monolayers treated with BFA early in the lag phase (*filled triangle*).

Table I. Distinct BFA-sensitive and Temperature-sensitive Events

Cholera Toxin Treatment	Time of Brefeldin A Treatment	15°C Temperature Block		Warm Up (32°C)	
		dI_{sc}/dt	Peak I_{sc}	$dI_{sc/dt}$	Peak I_{sc}
		$\mu A/cm^2$ per min	$\mu A/cm^2$	$\mu A/cm^2$ per min	$\mu A/cm^2$
Basolateral CT					
$n = 7$	None	0.03±0.01	7.9±0.6	0.12±0.004	19±2
Apical CT					
$n = 7$	None	Not present	0.6±0.06	0.09±0.007	14±2
Apical CT					
$n = 7$	27.5 min	Not present	1.0±0.3	0.09±0.04	8±2
Apical CT					
$n = 7$	0 min	Not present	0.2±0.3	Not present	1.0±0.3
None					
$n = 7$	27.5 min	Not present	0.3±0.05	Not present	0.9±0.2

ature-sensitive step that was not necessary for the action of basolateral CT. This temperature-sensitive event occurred late in the lag phase after formation of the A_1-peptide (19). In contrast, the rate limiting BFA-sensitive event described in this study occurred early in the lag phase before formation of the A_1-peptide. To distinguish more clearly between these events, we examined the time course of CT-induced Cl^- secretion after shifting monolayers to nonpermissive temperatures late in the lag phase in the presence or absence of BFA (5 μM) (Fig. 9). T84 monolayers exposed initially to apical or basolateral CT at 4°C, were preincubated at 37°C for 27.5 min to allow endocytosis and A-subunit translocation and returned to nonpermissive temperatures (13°–15°C). Those monolayers exposed to apical CT were either treated with BFA late (at 27.5 min, after preincubation at 37°C) or early (at 0 min, before preincubation at 37°C) in the lag phase. Control monolayers exposed to apical CT were not treated with BFA.

As previously reported, after shifting monolayers to nonpermissive temperatures, basolateral CT induced a Cl^- secretory response (dI_{sc}/dt = 0.03±0.01 $\mu A/cm^2/min$; peak I_{sc} = 7.9±0.6 $\mu A/cm^2$, mean±SEM, $n = 7$) but the action of apical CT (in the presence or absence of BFA) was completely inhibited even after 325 min (dI_{sc}/dt = not present; peak I_{sc} = 0.6 to 1.0 $\mu A/cm^2$). In monolayers treated with apical CT, rewarming to 32°C (at 325 min) restored toxin-induced Cl^- secretion in those monolayers not treated with BFA (dI_{sc}/dt = 0.09±0.007; peak I_{sc} = 14±2 $\mu A/cm^2$, $n = 7$) and in those monolayers treated with BFA late in the lag phase though the peak response was attenuated by the addition of BFA at 27.5 min (dI_{sc}/dt = 0.09±0.04; peak I_{sc} = 8±2 $\mu A/cm^2$, $n = 7$). In contrast, rewarming did not restore Cl^- secretion in monolayers treated with BFA early in the lag phase (dI_{sc}/dt = not present; peak I_{sc} = 1.0±0.3 $\mu A/cm^2$, $n = 7$) or in control monolayers not exposed to CT (dI_{sc}/dt = not present; peak I_{sc} = 0.9±0.2 $\mu A/cm^2$, $n = 7$). The viability of these nonsecreting monolayers was demonstrated by the brisk secretory response elicited by VIP at 400 min (dI_{sc}/dt = 11±4.6 $\mu A/cm^2/min$; peak I_{sc} = 20±1.5 $\mu A/cm^2$).

Table I summarizes the results of these experiments. In the absence of a temperature block, monolayers treated with BFA late in the lag phase would normally respond to apical CT with a strong secretory response (see Fig. 3). However, when monolayers were also shifted to nonpermissive temperatures late in the lag phase at the time of BFA treatment (at 27.5 min) toxin-induced Cl^- secretion was completely inhibited. The data show that two sequential and distinct events, comprised of an early lag phase BFA-sensitive event followed by a late lag phase temperature-sensitive event, are essential for toxin-induced signal transduction from the apical membrane. This was demonstrated directly by rewarming to permissive temperatures at 325 min, which released the temperature block and elicited a toxin-induced secretory response in those monolayers treated with BFA late in the lag phase (at 27.5 min) but not in those monolayers treated with BFA early in the lag phase (at 0 min).

Discussion

In this report, using the fungal metabolite BFA, we identify an event involving vesicular transport that is required for a biologic response to apical CT and that is distinct from the late lag phase temperature-sensitive vesicular transport event previously described (19). The BFA-sensitive event occurs early in the lag phase and involves the transport of CT to a site beyond the early endosome where the A-subunit is reduced to the A_1-peptide. The data strongly suggest that in polarized epithelia, vesicular transport through multiple compartments of membranes containing CT (and possibly also ADP-ribose-Gsα) play an essential role in the mechanism of toxin-induced signal transduction.

Brefeldin A as a probe of vesicular transport in the mechanism of CT action. Brefeldin A has structural and functional effects on the endoplasmic reticulum, the Golgi complex, the endosomal system and the trans-Golgi network of a variety of cell types (23, 24, 25, 40, 41). The drug appears to act by interfering with the regulated assembly of specific cytosolic coat proteins required for the budding and transport of vesicular carriers associated with these organelles (27, 42, 43, 44, 45). As a result, BFA disrupts the steady-state distribution of membranes and membrane components, and organelle identity and function are altered. At the cellular level, disruption of vesicular transport by BFA has been shown to strongly inhibit protein secretion from hepatocytes (46) and MDCK cells (47); antigen presentation by MHC class-I and -II molecules on B-cell hybridomas (48, 49); ganglioside biosynthesis in primary cultured cerebellar cells (50); cytotoxicity of ricin, modeccin, and *Pseudomonas* toxins in CHO, Vero, and NRK cells (51); and transcytosis of the polymeric immunoglobulin receptor in MDCK cells (25). In many of these cell systems, however,

endocytosis and rapid recycling of specific membrane components to the cell surface were not affected (24, 25, 46, 51). We found that T84 cells are also sensitive to BFA since, like in many of the systems described above, Golgi structure was perturbed by the drug as assessed by the redistribution of the Golgi-specific coat protein p200 (36).

In this report, we show that brefeldin A completely and reversibly inhibited CT-induced Cl^- secretion in the epithelial cell line T84. In contrast, BFA did not inhibit Cl^- secretion induced by other agonists, which activated $Gs\alpha$ via a basolateral cell surface peptide receptor or which directly activated A-kinase or adenylate cyclase. Not only was inhibition of the Cl^- secretory response by BFA specific for CT, but this inhibition was only manifested on intact cells. For example, BFA did not inhibit the reduction of the CT A-subunit to the enzymatically active A_1-peptide when CT and extracted cytosol were coincubated in the presence of this drug. Furthermore, BFA did not inhibit the A_1-peptide catalyzed ADP-ribosylation of $Gs\alpha$ in membrane fractions of T84 cells. The data indicate that CT action on intact T84 cells requires BFA-sensitive steps unique from other cAMP-mediated secretagogues, and that BFA does not block CT action by interfering with the toxin's ADP-ribosyltransferase activity.

Effect of epithelial cell polarity on the mechanism of CT action. We have previously shown that the time course and temperature-sensitivity of the secretory response to apical CT in T84 cell monolayers was different from that of CT applied to basolateral membranes of the same cells (19). In this report, we show that the secretory response elicited by apical CT also differed in sensitivity to BFA. Our data indicate that BFA acts at an early stage in the lag phase for both apical and basolateral CT and suggest that signal transduction by basolateral CT may also involve endocytosis and vesicular transport of CT-containing membranes. These data are consistent with studies reported while this manuscript was under review, that BFA effects CT action on nonpolarized cells (29, 30). In the polarized T84 cell model, however, we find that the half-time for transit through a BFA-sensitive compartment was significantly longer for CT bound to apical cell surfaces. In addition, we found that the secretory response elicited by apical CT was almost twofold more sensitive to BFA than the secretory response elicited by basolateral CT. These differences in time and dose dependency suggest that BFA may inhibit CT-induced Cl^- secretion by acting at similar but not necessarily identical site(s) in the apical and basolateral endocytic pathways. Indeed, available evidence from a variety of other cell systems indicate that BFA may have specific effects at multiple sites within the central vacuolar system of a single cell type (25, 28, 52, 53). Taken together, our studies suggest that the mechanism of toxin action from the apical (or physiologic) cell surface entails additional steps (temperature-sensitivity late in the lag phase), steps of longer duration, and steps with differing sensitivity to BFA than that required from the basolateral cell surface. Since CT action has previously been examined in nonpolarized cell systems, these observations also suggest that the pathway of signal transduction seen in nature may entail complexities not previously appreciated.

Mechanism of BFA-action at the membrane surface: the role of ADP-ribosylating factors in CT-induced signal transduction. The mechanism of BFA-action has been most extensively studied by examining the drug's effect on Golgi membranes (27, 42, 43–45, 54–56). These studies show that brefeldin A may act by interfering with the GTP-dependent assembly of specific coat proteins required for the budding and transport of vesicular carriers between Golgi stacks. The data indicate that a family of small molecular weight GTP-binding proteins, termed ADP-Ribosylating Factors (ARF), play a fundamental role in GTP-dependent coat assembly (57–60). GDP/GTP exchange redistributes ARF between membrane-associated and cytosolic forms (61, 62). Movement of ARF onto Golgi membranes appears to be a prerequisite for the assembly of coat proteins on nascent transport vesicles (57), and recent evidence, from two independent laboratories, indicate that this process may be catalyzed by a BFA-sensitive Golgi membrane associated GDP/GTP exchange factor (63, 64).

It is not known whether BFA interferes with vesicular transport between other organelles by acting on ARF or related exchange factors located at different sites within the endocytic and exocytic pathways. However, convincing data now indicate that ARF proteins are required for vesicular traffic in *Saccharomyces cerevisiae* (59) and play an important role in regulating vesicular traffic between ER and Golgi (65), within the endosomal compartment (66), as well as between Golgi cisternae (67) in mammalian cells. These studies raise the possibility that ARF may play a role in the BFA-sensitive event required for transport of CT beyond the early apical endosomal compartment in T84 cells. If so, this would be particularly relevant because the ARF protein family was initially identified based on the ability of ARF to act as potent allosteric activators of CT actions in vitro (68). One might even speculate that CT has evolved to facilitate its own movement through the endocytic pathway by interacting with ARF. In our in vitro assay of toxin ADP-ribosyl-transferase activity, we found that CT catalyzed the ADP-ribosylation *a* 20-kD protein present in T84 cell membrane pellets (Fig. 7, * at 20 kD). Since CT is known to ADP-ribosylate ARF in vitro (69), we sought to determine the identity of this 20-kD membrane protein. However, although this protein had an identical electrophoretic mobility on SDS-PAGE to cytosolic ARF it was not clearly immunoreactive with polyclonal antibodies against ARF as assessed by western blot (data not shown; antibodies obtained from Dr. Joel Moss, National Institutes of Health, Bethesda, MD).

Sequential BFA- and temperature-sensitive events are required for signal transduction from the apical membrane. These studies have functionally identified two sequential events required for a biologic response to apical CT (Fig. 10). Both events occur after binding to apical cell surfaces and after entry into an apical endocytic compartment. The first event occurs early in the lag phase and involves BFA-sensitive transport of CT to an intracellular compartment where reduction of the A-subunit (and possibly translocation) occurs. The second event occurs late in the lag phase and involves temperature-sensitive signal transduction (presumably via the A_1-peptide but possibly via ADP-ribose-$Gs\alpha$) to the basolateral domain. This late lag phase temperature-sensitive event was apparent only when CT was applied to apical (physiologic) cell surfaces (19).

Though the exact intracellular compartments associated with these events are not yet known, the data strongly support a role for multi-compartmental vesicular traffic in the mechanism of toxin action. Based on our current understanding, we propose the following working model. CT-induced signal transduction from apical membranes of polarized T84 cells requires toxin entry into the early apical endosomal compartment. Movement of toxin-containing membranes out of the early endosome to the late endosome or possibly to the *trans-*

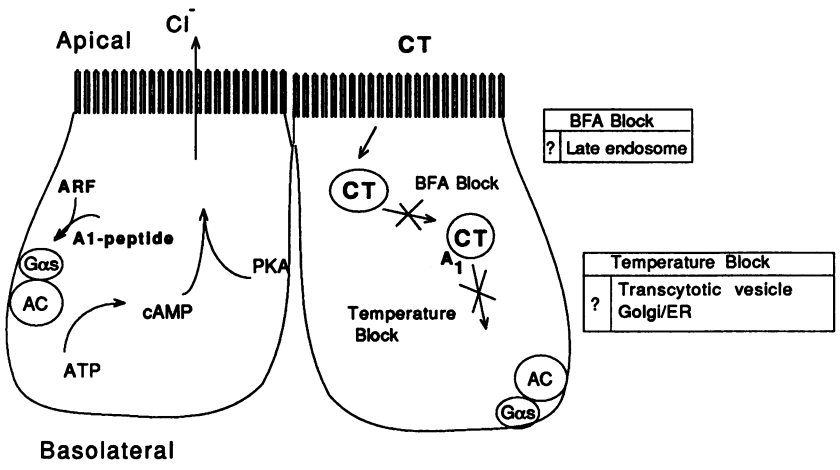

Figure 10. Proposed model for mechanism of CT action on polarized epithelia. Sequential events are required for signal transduction from the apical membrane: (*a*) binding to cell surfaces and rapid endocytosis; (*b*) early, BFA-sensitive vesicular transport essential for reduction of the A_1 peptide; and (*c*) subsequent temperature-sensitive translocation of a signal (the A_1-peptide or possibly ADP-ribose-Gsα) to the basolateral domain. AC, adenylate cyclase. Gsα, heterotrimeric GTPase Gsα. ARF, ADP-ribosylating factor. PKA, protein kinase A. CT, cholera toxin. A_1, CT-A_1-peptide.

Golgi requires BFA-sensitive and probably ARF-mediated vesicular transport. Translocation of the A-subunit occurs in a compartment distal to the early endosome. Signal transduction to basolateral adenylate cyclase may occur by entry of the A_1-peptide into vesicles targeted to the basolateral membrane or by dissociation of the A_1-peptide from the membrane and diffusion in the cytosol at some point after translocation. Alternatively, the A-subunit may translocate in a compartment containing Gsα. We have no direct evidence that retrograde transit through an intact Golgi is required for toxin action, though this is a distinct possibility suggested by the sensitivity of T84 Golgi structures to treatment with BFA and by the presence of the ER-targeting signal KDEL at the COOH-terminus of the A_2-peptide (5, 70). If so, the A_1-peptide could catalyze the ADP-ribosylation of Gsα during its transit through the Golgi or *trans*-Golgi complex (71). Signal transduction to adenylate cyclase on the basolateral membrane may then be mediated by movement of ADP-ribose-Gsα, the toxin-Gsα complex, or both.

Since CT has an apical membrane receptor (ganglioside G_{M1}) but a basolateral effector (adenylate cyclase), signal transduction by apically bound CT may represent a paradigm for the study of targeted protein movement through polarized epithelia. If so, elucidating the molecular mechanisms specific to the endocytosis and transport of CT-containing membranes may lead to further clarification of these fundamental aspects of epithelial cell biology.

Acknowledgments

We thank Marian R. Neutra for critical reading of the manuscript and Paul Knoephlmacher, Charlene Archer-Delp, and Susan Carlson for expert technical assistance.

This work was supported by National Institutes of Health research grants DK48106 (W. I. Lencer), DK35932, DK33506 (J. L. Madara), DK38452 (D. A. Ausiello), and Harvard Digestive Diseases Center grant DK34854. W. I. Lencer is recipient of Clinical Investigator Award KO8-DK01848.

References

1. Donowitz, M., and M. J. Welsh. 1987. Regulation of mammalian small intestinal electrolyte secretion. *In* Physiology of the Gastrointestinal Tract. J. R. Johnson, editor. Raven Press, New York. 1351–1388.

2. Cassuto, J., M. Jodal, and O. Lundgren. 1981. On the role of intramural nerves in the pathogenesis of cholera toxin-induced intestinal secretion. *Scand. J. Gastroent.* 16:377–384.

3. Peterson, J. W., and L. G. Ochoa. 1989. Role of prostaglandins and cAMP in the secretory effects of cholera toxin. *Science (Wash. DC).* 245:857–859.

4. Halm, D. R., and R. A. Frizzell. 1990. Intestinal chloride secretion. *In* Textbook of Secretory Diarrhea. E. Lebenthal and M. E. Duffey, editors. Raven Press, New York. 47–58.

5. Sixma, T. K., S. E. Pronk, H. H. Kalk, E. S. Wartna, B. A. M. van Zanten, B. Witholt, and W. G. J. Hol. 1991. Crystal structure of a cholera toxin-related heat-labile enterotoxin from E. coli. *Nature (Lond.).* 351:371–377.

6. Fishman, P. H. 1980. Mechanism of action of cholera toxin: Studies on the lag period. *J. Membr. Biol.* 54:61–72.

7. Dominguez, P., G. Velasco, F. Barros, and P. S. Lazo. 1987. Intestinal brush border membranes contain regulatory subunits of adenyl cyclase. *Proc. Natl. Acad. Sci. USA.* 84:6965–6969.

8. Murer, H., E. Ammann, J. Biber, and U. Hopfer. 1976. The surface membrane of the small intestinal epithelial cell—Localization of adenyl cyclase. *Biochim. Biophys. Acta.* 433:509–519.

9. Peterson, J. W., J. J. LoSpalluto, and R. A. Finkelstein. 1972. Localization of cholera toxin in vivo. *J. Inf. Dis.* 126:617–628.

10. Spiegel, S., R. Blumenthal, P. Fishman, and J. S. Handler. 1985. Gangliosides do not move from apical to basolateral plasma membrane in cultured epithelial cells. *Biochim. Biophys. Acta.* 821:310–318.

11. Fishman, P. H. 1990. Mechanism of action of cholera toxin. *In* ADP-Ribosylating Toxins and G-Proteins. J. Moss and M. Vaughan, editors. American Society for Microbiology, Washington, DC. 127–140.

12. Janicot, M., F. Fouque, and B. Desbuquois. 1991. Activation of rat liver adenylate cyclase by cholera toxin requires toxin internalization and processing in endosomes. *J. Biol. Chem.* 266:12858–12865.

13. Kassis, S., J. Hagmann, P. H. Fishman, P. P. Chang, and J. J. Moss. 1982. Mechanism of action of cholera toxin on intact cells: Generation of A1 peptide and activation of adenylate cyclase. *J. Biol. Chem.* 257:12148–12152.

14. Ribi, H. O., D. S. Ludwig, K. L. Mercer, G. K. Skoolnik, and R. D. Kornberg. 1988. Three dimensional structure of cholera toxin penetrating a lipid membrane. *Science (Wash. DC).* 239:1272–1276.

15. Wisnieski, B. J., and J. S. Bramhall. 1981. Photolabeling of cholera toxin subunits during membrane penetration. *Nature (Lond.).* 289:319–321.

16. Cassel, D., and Z. Selinger. 1977. Mechanism of adenylate cyclase activation by cholera toxin: Inhibition of GTP hydrolysis at the regulatory site. *Proc. Natl. Acad. Sci. USA.* 74:3307–3311.

17. Moss, J., and M. Vaughan. 1977. Mechanism of action of choleragen: Evidence for ADP-ribosyltransferase activity with arginine as an acceptor. *J. Biol. Chem.* 252:2455–2457.

18. Longbottom, D., and S. van Heyningen. 1989. The activation of rabbit intestinal adenylate cyclase by cholera toxin. *Biochim. Biophys. Acta.* 1014:289–297.

19. Lencer, W. I., C. Delp, M. R. Neutra, and J. L. Madara. 1992. Mechanism of cholera toxin action on a polarized human epithelial cell line: role of vesicular traffic. *J. Cell Biol.* 117:1197–1209.

20. Joseph, K. C., A. Stieber, and N. K. Gonatas. 1979. Endocytosis of cholera toxin in GERL-like structures of murine neuroblastoma cells pretreated with GM1 ganglioside. *J. Cell Biol.* 81:543–554.

21. Montesanto, R., J. Roth, and L. Orci. 1982. Non-coated membrane invaginations are involved in binding and internalization of cholera and tetanus toxins. *Nature (Wash. DC).* 296:651–653.

22. Fishman, P. H. 1982. Internalization and degradation of cholera toxin by cultured cells: relationship to toxin action. *J. Cell Biol.* 93:860–865.

23. Wood, S. A., J. E. Park, and W. J. Brown. 1991. Brefeldin A causes a microtubule-mediated fusion of the trans-Golgi network and early endosomes. *Cell.* 67:591–600.

24. Lippincott-Schwartz, J., L. Yuan, C. Tipper, M. Amherdt, L. Orci, and R. D. Klausner. 1991. Brefeldin A's effects on endosomes, lysosomes, and the

TGN suggest a general mechanism for regulating organelle structure and membrane traffic. *Cell.* 67:601–616.

25. Hunziker, W., J. A. Whitney, and I. Mellman. 1991. Selective inhibition of transcytosis by brefeldin A in MDCK cells. *Cell.* 67:617–627.

26. Fujiwara, T., K. Oda, S. Yokota, A. Takatsuki, and Y. Ikehara. 1988. Brefeldin A causes disassembly of the Golgi complex and accumulation of secretory proteins in the endoplasmic reticulum. *J. Biol. Chem.* 263:18545–18552.

27. Klausner, R. D., J. G. Donaldson, and J. Lippincott-Schwartz. 1992. Brefeldin A: insights into the control of membrane traffic and organelle structure. *J. Cell Biol.* 116:1071–1080.

28. Pelham, H. R. B. 1991. Multiple targets for brefeldin A. *Cell.* 67:449–451.

29. Nambiar, M. P., T. Oda, C. Chen, Y. Kuwazuru, and H. C. Wu. 1993. Involvement of the Golgi region in the intracellular trafficking of cholera toxin. *J. Cell Physiol.* 154:222–228.

30. Orlandi, P. A., P. K. Curran, and P. H. Fishman. 1993. Brefeldin A blocks the response of cultured cells to cholera toxin, implications for intracellular trafficking in toxin action. *J. Biol. Chem.* 268:12010–12016.

31. Dharmsathaphorn, K., and J. L. Madara. 1990. Established intestinal cell lines as model systems for electrolyte transport studies. *Methods Enzymol.* 192:354–359.

32. Madara, J. L., S. Colgan, A. Nusrat, C. Delp, and C. Parkos. 1992. A simple approach to measurement of electrical parameters of cultured epithelial monolayers. *J. Tiss. Cult. Tech.* 14:209–216.

33. Madara, J. L., and K. Dharmsathaphorn. 1985. Occluding junction structure-function relationships in a cultured epithelial monolayer. *J. Cell Biol.* 101:2124–2133.

34. Lencer, W. I., S. H. Chu, and W. A. Walker. 1987. Differential binding kinetics of cholera toxin to developing intestinal microvillus membrane. *Infect. Immun.* 55:3126–3130.

35. Le Bivic, A., Y. Sambuy, K. Mostov, and E. Rodriguez-Boulan. 1990. Vectorial Targeting of an endogenous apical membrane sialoglycoprotein and uvomorulin in MDCK cells. *J. Cell Biol.* 110:1533–1539.

36. Narula, N., I. McMorrow, G. Plopper, J. Doherty, K. S. Matlin, B. Burke, and J. L. Stow. 1992. Identification of a 200-kD, brefeldin-sensitive protein on Golgi membranes. *J. Cell Biol.* 117:27–38.

37. Kaoutzani, P., C. A. Parkos, C. Delp-Archer, and J. L. Madara. 1993. Isolation of plasma membrane fractions from the intestinal epithelial model T84. *Am. J. Physiol. (Cell).* 264:C1327–C1335.

38. Ribeirto-Neto, F. A., R. Mattera, J. D. Hildebrant, J. Codina, J. B. Field, L. Birnbaumer, and R. D. Sehura. 1985. ADP-ribosylation of membrane components by pertussis and cholera toxin. *Methods Enzymol.* 109:566–572.

39. Zizi, M., R. S. Fisher, and F. G. Grillo. 1991. Formation of cation channels in planar lipid bilayers by brefeldin A. *J. Biol. Chem.* 266:18443–18445.

40. Reaves, B., and G. Banting. 1992. Perturbation of the morphology of the trans-Golgi network following brefeldin A treatment: redistribution of a TGN-specific integral membrane protein, TGN38. *J. Cell Biol.* 116:85–94.

41. Lippincott-Schwartz, J., L. C. Yuan, J. S. Bonifacino, and R. D. Klausner. 1989. Rapid distribution of Golgi proteins into the ER in cells treated with brefeldin A: evidence for membrane recycling from Golgi to ER. *Cell.* 56:801–813.

42. Donaldson, J. G., J. Lippincott-Schwartz, G. S. Bloom, T. E. Kreis, and R. D. Klausner. 1990. Dissociation of a 110-kD peripheral membrane protein from the Golgi apparatus is an early event in brefeldin A action. *J. Cell Biol.* 111:2295–2306.

43. Donaldson, J. G., J. Lippincott-Schwartz, and R. D. Klausner. 1991. Guanine nucleotides modulate the effects of brefeldin A in semipermeable cells: regulation of the association of a 110-kD peripheral membrane protein with the Golgi apparatus. *J. Cell Biol.* 112:579–588.

44. Orci, L., M. Tagaya, M. Amherdt, A. Perrelet, J. G. Donaldson, J. Lippincott-Schwartz, R. D. Klausner, and J. E. Rothman. 1991. Brefeldin A, a drug that blocks secretion, prevents the assembly of non-clathrin-coated buds on Golgi cisternae. *Cell.* 64:1183–1195.

45. Robinson, M. S., and T. E. Kreis. 1992. Recruitment of coat proteins onto Golgi membranes in intact and permeabilized cells: effects of brefeldin A and G protein activators. *Cell.* 69:129–138.

46. Misumi, Y., Y. Misumi, K. Miki, A. Takatsuki, G. Tamura, and Y. Ikehara. 1986. Novel blocade by brefeldin A of intracellular transport of secretory proteins in cultured rat hepatocytes. *J. Biol. Chem.* 261:11398–11403.

47. Low, S. H., S. H. Wong, B. L. Tang, P. Tan, V. N. Subramaniam, and W. Hong. 1991. Inhibition by brefeldin A of protein secretion from the apical cell surface of Madin-Darby canine kidney cells. *J. Biol. Chem.* 266:17729–17732.

48. Nuchtern, J. G., W. E. Biddison, and R. D. Klausner. 1990. Class II MHC molecules can use the endogenous pathway of antigen presentation. *Nature (Lond.).* 343:74–76.

49. Adorini, L., S. J. Ullrich, E. Appella, and S. Fuchs. 1990. Inhibition by brefeldin A of presentation of exogenous protein antigens to MHC class II-restricted T cells. *Nature (Lond.).* 346:63–66.

50. van Echten, G., H. Iber, H. Stotz, A. Takatusuki, and K. Sandhoff. 1990. Uncoupling of ganglioside biosynthesis by brefeldin A. *Eur. J. Cell. Biol.* 51:135–139.

51. Yoshida, T., C. Chen, M. Zhang, and H. C. Wu. 1991. Disruption of the Golgi apparatus by brefeldin A inhibits the cytotoxicity of ricin, modeccin, and *Pseudomonas* toxin. *Exp. Cell Res.* 192:389–395.

52. Strous, G. J., P. van Kerkhof, G. van Meer, S. Rijnboutt, and W. Stoorvogel. 1993. Differential effects of brefeldin A on transport of secretory and lysosomal proteins. *J. Biol. Chem.* 268:2341–2347.

53. Low, S. H., B. L. Tang, S. H. Wong, and W. Hong. 1992. Selective inhibition of protein targeting to the apical domain of MDCK cells by brefeldin A. *J. Cell Biol.* 118:51–62.

54. Lippincott-Schwartz, J., J. Glickman, J. G. Donaldson, J. Robbins, T. E. Kreis, K. B. Seamon, M. P. Sheetz, and R. D. Klausner. 1991. Forskolin inhibits and reverses the effects of brefeldin A on Golgi morphology by a cAMP-independent mechanism. *J. Cell Biol.* 112:567–577.

55. Ktistakis, N. T., M. G. Roth, and G. S. Bloom. 1991. PtK1 cells contain a nondiffusible, dominant factor that makes the Golgi apparatus resistant to brefeldin A. *J. Cell Biol.* 113:1009–1023.

56. Ktistakis, N. T., M. E. Linder, and M. G. Roth. 1992. Action of brefeldin A blocked by activation of a pertussis-toxin-sensitive G protein. *Nature (Lond.).* 356:344–346.

57. Donaldson, J. G., D. Cassel, R. A. Kahn, and R. A. Klausner. 1992. ADP-ribosylation factor, a small GTP-binding protein, is required for binding of the coatomer protein B-COP to Golgi membranes. *Proc. Natl. Acad. Sci. USA.* 89:6408–6412.

58. Donaldson, J. G., R. A. Kahn, J. Lippincott-Schwartz, and R. D. Klausner. 1991. Binding of ARF and B-COP to golgi membranes: possible regulation by a trimeric G protein. *Science (Wash. DC).* 254:1197–1199.

59. Stearns, T., M. C. Willingham, D. Botstein, and R. A. Kahn. 1990. ADP-ribosylation factor is functionally and physically associated with the Golgi complex. *Proc. Natl. Acad. Sci. USA.* 87:1238–1242.

60. Taylor, T. C., R. A. Kahn, and P. Melancon. 1992. Two distinct members of the ADP-ribosylation factor family of GTP-binding proteins regulate cell-free intra-Golgi transport. *Cell.* 70:69–79.

61. Walker, M. W., D. A. Bobak, S-C. Tsai, J. Moss, and M. Vaughan. 1992. GTP but not GDP analogues promote association of ADP-ribosylation factors, 20-kDa protein activators of cholera toxin, with phospholipids and PC-12 cell membranes. *J. Biol. Chem.* 267:3230–3235.

62. Regazzi, R., S. Ullrich, R. A. Kahn, and C. B. Wollheim. 1991. Redistribution of ADP-ribosylation factor during stimulation of permeabilized cells with GTP analogues. *Biochem. J.* 275:639–644.

63. Donaldson, J. G., D. Finazzi, and R. D. Klausner. 1992. Brefeldin A inhibits Golgi membrane-catalysed exchange of guanine nucleotide onto ARF protein. *Nature (Lond.).* 360:350–352.

64. Helms, J. B., and J. E. Rothman. 1992. Inhibition by brefeldin A of a Golgi membrane enzyme that catalyses exchange of guanine nucleotide bound to ARF. *Nature (Lond.).* 360:352–354.

65. Balch, W. E., R. A. Kahn, and R. Schwaninger. 1992. ADP-ribosylation factor is required for vesicular trafficking between the endoplasmic reticulum and the *cis*-Golgi compartment. *J. Biol. Chem.* 267:13053–13061.

66. Lenhard, J. M., R. A. Kahn, and P. D. Stahl. 1992. Evidence for ADP-ribosylation factor (ARF) as a regulator of in vitro endosome-endosome fusion. *J. Biol. Chem.* 267:13047–13052.

67. Kahn, R. A., P. Randazzo, T. Serafini, O. Weiss, C. Rulka, J. Clark, M. Amherdt, P. Roller, L. Orci, and J. E. Rothman. 1992. The amino terminus of ADP-ribosylation factor (ARF) is a critical determinant of ARF activities and is a potent and specific inhibitor of protein transport. *J. Biol. Chem.* 267:13039–13046.

68. Kahn, R. A., and A. G. Gilman. 1984. Purification of a protein cofactor required for ADP-ribosylation of the stimulatory regulatory component of adenylate cyclase by cholera toxin. *J. Biol. Chem.* 259:6228–6234.

69. Tsai, S-C., M. Noda, R. Adamik, J. Moss, and M. Vaughan. 1987. Enhancement of choleragen ADP-ribosyltransferase activities by guanyl nucleotides and a 19-kDa membrane protein. *Proc. Natl. Acad. Sci. USA.* 84:5139–5142.

70. Pelham, H. R. B., L. M. Roberts, and M. Lord. 1992. Toxin entry: how reversible is the secretory pathway. *Trends Cell Biol.* 2:183–185.

71. Pimplikar, S. W., and K. Simons. 1993. Regulation of apical transport in epithelial cells by a Gs class of heterotrimeric G protein. *Nature (Lond.).* 362:456–458.